

The Fracture Toughness of Composites Reinforced with Weakened Fibres

G. A. COOPER

Division of Inorganic and Metallic Structure, National Physical Laboratory, Teddington, Middx, UK

Fibre fractures which occur near, but not at, the plane of matrix failure in a composite, lead to fibre pull-out during fracture. Energy absorbed in this process contributes directly to the work of fracture and hence to the toughness of the composite.

Factors which determine the mean length of fibre pulled out during fracture are discussed for the case of composites reinforced with continuous fibres having variously spaced points of weakness. The presence of such weak points also affects the strength of the composite, but not all composites of the same strength have the same toughness. The greatest toughness for a given strength is always found in composites reinforced with discontinuous fibres.

1. Introduction

When a composite reinforced with parallel, discontinuous fibres is subjected to tension parallel with the fibre axes, failure can occur either by pulling-out or by fracture of the fibres. A single fibre, considered in isolation, is expected to pull out if one end is within a distance $l_c/2$ of the fracture plane of the matrix, where l_c is the "critical length". If not, the fibre will be broken.

Following this argument, and neglecting interactions between fibres, Cottrell [1] and Kelly [2] have shown that composites reinforced with discontinuous fibres fall into two classes, being either (i) those in which the fibres are of length less than l_c , in which case no fibre is broken during fracture of the composite, or (ii) those in which the fibre length (l) is greater than l_c . In this case, a fraction l_c/l of the fibres will be pulled out, while the others will be broken.

A composite reinforced with parallel, continuous fibres which have no weak points is expected to fail on a plane normal to the fibre axis, and there will be no fibre pull-out.

Real composites often have properties between these two extremes, being reinforced by fibres which are continuous, but which have weak points from place to place along their length.

As a failure crack propagates through such a material, a fibre in the path of the crack will be broken either where it crosses the plane of the crack (i.e. where the stress is greatest) or at a flaw

in the fibre which is near, but not necessarily on, this plane. This latter behaviour gives rise to fibre pull-out during fracture, and contributes to the work of fracture. The tendency to failure at weak points is determined by their frequency and degree of weakness, so that these two parameters have a direct influence upon the mean length of fibre involved in the pulling-out process during fracture, and hence upon the fracture toughness of the composite.

The frequency and severity of the flaws also affect the strength of the composite, but not in the same way as their effect upon the fracture toughness.

It was the aim of the work described below to examine the effect of fibre flaw size and frequency upon composite strength and toughness, in order to obtain information about composites with flawed fibres (i.e. most composites with a brittle reinforcement) and to determine whether there exist particular combinations of properties which give increased toughness while at the same time maintaining a high strength.

2. Experimental

It is an almost impossible task to seek a reinforcing fibre which is completely brittle, yet which is also of a constant strength, and which can have weak points of known strength and spatial distribution in it. Experiments were therefore made on a system of phosphor-bronze wires in a

plasticised epoxy resin. Phosphor-bronze was chosen for the reinforcing fibre since it is very ductile, and can be cold-drawn to beyond its ultimate tensile stress. In this condition, the elongation to failure of a wire is only of the order of the wire diameter, since necking occurs at yield. Such material is, however, still sufficiently ductile for notches to be made in the wire (by nipping the wire between hardened jaws) with a high degree of reproducibility, and without danger of completely cutting the wire. The use of such wire ensured a high degree of repeatability in the strength of the "undamaged" wire, and also a close control of the strength of the flawed regions.

The "flaws" were introduced into the wire by passing it through an automatic guillotine having a moving knife edge cutting against a fixed flat surface. Micrometer adjustment of the position of the flat surface gave a variable depth of cut and hence a variable strength of "flaw". The wire was advanced through the machine in synchronisation with the movement of the guillotine by means of one moving and one fixed electromagnetic clamp. Fig. 1 shows the variation in the breaking load of 550 μm diameter wires for various settings of the guillotine micrometer. This diameter was used in all the experiments reported here.

The matrix resin was based on the "Araldite" system MY 750: HY 951 (Messrs CIBA Ltd). When cast without plasticiser, this resin is extremely brittle, and it is difficult to obtain consistent values for the shear strength of the wire: resin interface. More uniform values are obtained if the resin is plasticised, and so, in the main series of experiments, a system consisting of sixty parts by weight of "Araldite" MY750, forty parts plasticiser CY 208, and ten parts hardener HY 951 was used. The variation of resin properties with plasticiser content is shown in figs. 2 and 3.

3. Fibre Pull-out Tests

Data on the strength of the fibre: resin interface were obtained from single wire pull-out tests by measuring the load necessary to withdraw a single wire from a block of the matrix resin. Both the failure load of the interface and the sliding friction stress during pull-out were measured.

Examination of these specimens between crossed polaroids showed the presence of a variable degree of strain in the resin after curing. The fringes were always associated with the wire, being most dense near its end. The effect was most noticeable in specimens which had been cured at high temperatures, and these also showed high values of the interfacial strength. It

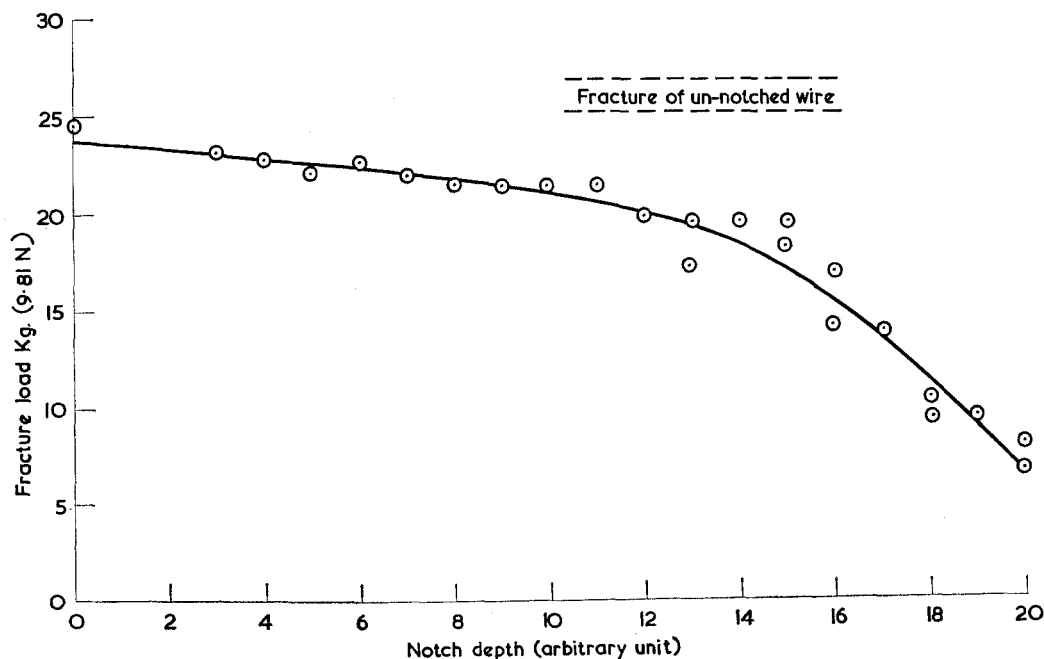


Figure 1 Variation of failure load with guillotine setting for phosphor-bronze wires of 550 μm diameter.

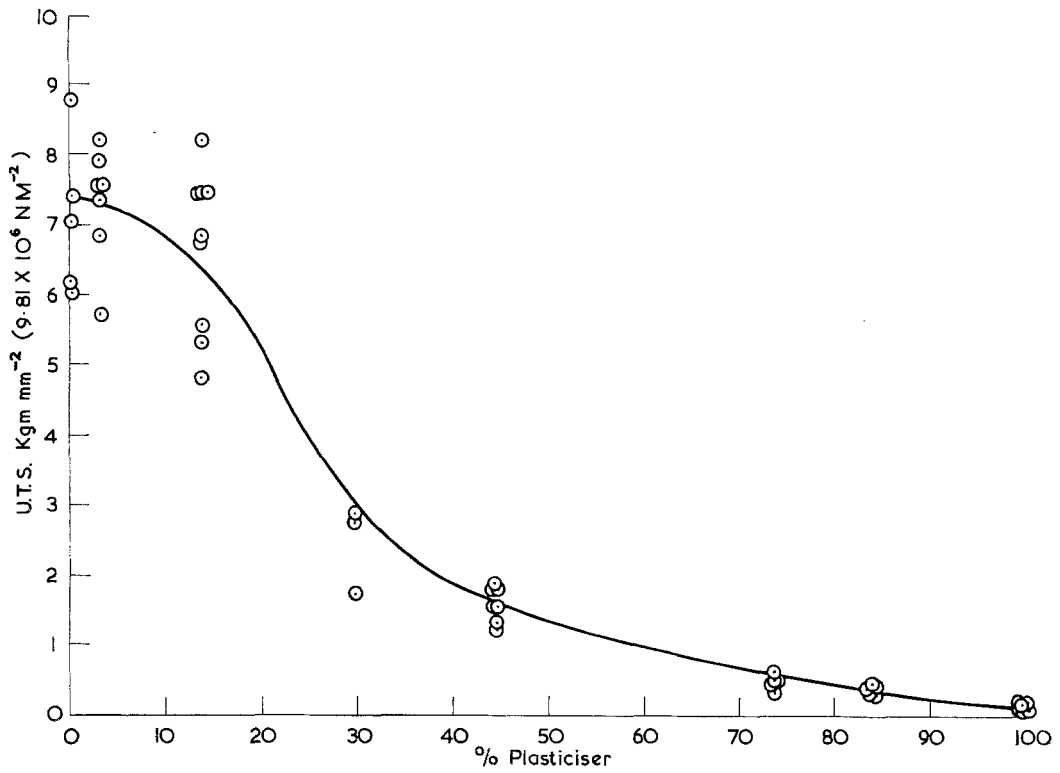


Figure 2 Variation of resin strength with plasticiser content: loading rate 0.05 cm min⁻¹ at 20° C.

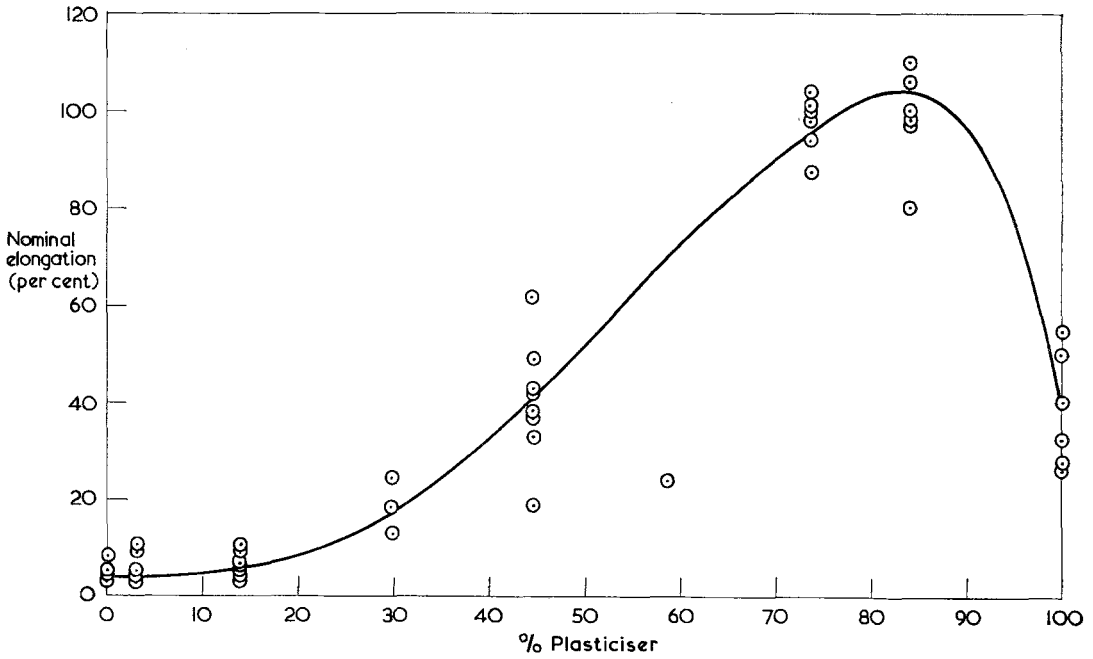


Figure 3 Variation of resin ductility with plasticiser content: loading rate 0.05 cm min⁻¹ at 20° C.

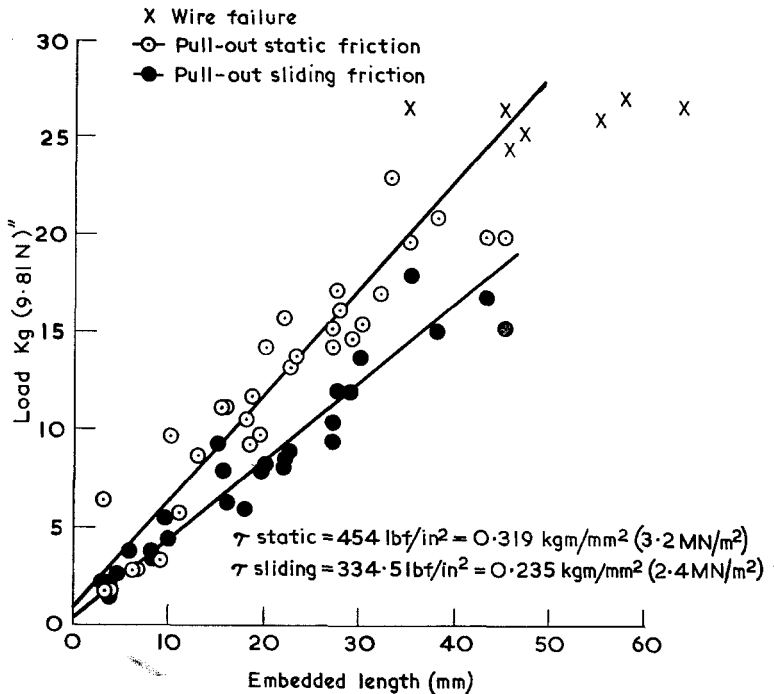


Figure 4 Variation of load necessary to cause failure of the resin-fibre interface (upper) and the sliding friction load during pull-out (lower) as a function of embedded length of wire.

was concluded that the effect was caused by differential thermal contraction between wire and resin on cooling from the curing temperature, and so in all the experiments described below, a close control of resin curing conditions was maintained, as follows: (i) weigh out required quantities of resin, hardener and plasticiser, warm to 60°C to allow bubbles to rise and burst, (ii) cool to 45°C , mix and pour into moulds, (iii) allow to harden for 12 h at 20°C , (iv) extract mouldings and post-cure by placing in an oven at 100°C , then cool over 12 h to room temperature. In this way consistent resin properties were developed in most specimens. Values of static and sliding loads to pull out wires embedded to different depths in the matrix are shown in fig. 4.

4. Tensile Testing of Composites

Various trials were made to obtain a tensile specimen which showed a consistent and reproducible single-plane fracture. The final design is shown in fig. 5 (top). The specimens, of overall dimensions $20 \times 2 \times 1$ cm, were made in a mould provided with two wedge-shaped fillers, and the reinforcing wires were laid along the length of the mould between them. The aim of this design was to provide an encouragement for the matrix to fail on the mid-plane of the speci-

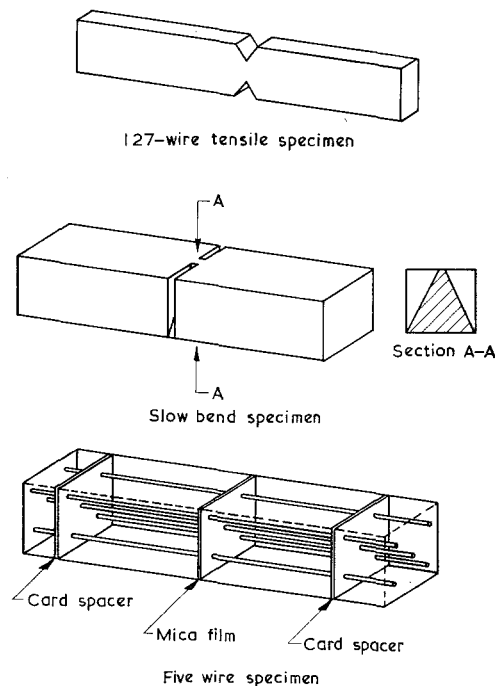


Figure 5 Shapes of test specimen.

men, yet to avoid the presence of a large number of cut fibres in the region of the failure, which would have been the case if notches were sawn

out after casting. The number of wires in each specimen was chosen to be 127 in order to give a volume fracture of exactly 30% fibres in the region of fracture.

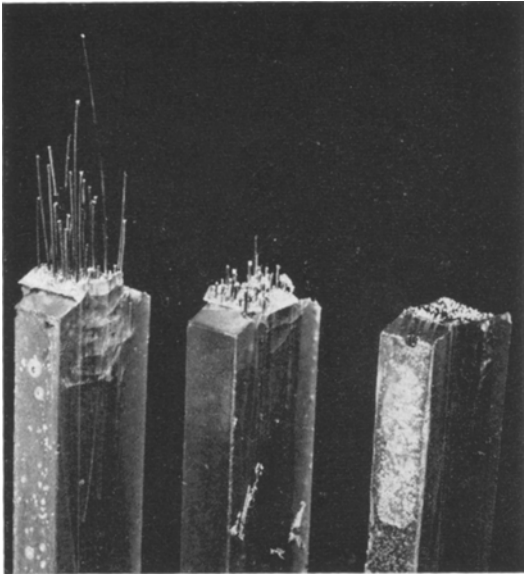


Figure 6 Appearance of fracture surfaces of the tensile specimens: (a) $\sigma^*/\sigma = 0$, $d = 10$ mm; (b) $\sigma^*/\sigma = 0.41$, $d = 20$ mm; (c) un-notched wire.

Specimens were gripped between wedge-grips in an "Instron", tensile testing machine and loaded at a rate of elongation of 0.05 cm min^{-1} . In most cases, a single-plane fracture occurred in the resin matrix, varying degrees of fibre pull-out being observed, depending upon the arrangement of weak points in the reinforcing wires (fig. 6).

Specimens were made having various values of flaw spacing (d) and strength of flawed region (σ^*), the values of d and σ^* being kept constant in any one specimen, although the position of the weak points was made random from wire to wire across the width of the specimen. In fig. 7, failure load is shown plotted against d for various values of σ^*/σ , i.e. the ratio of the effective strength of a notched region to that of the unnotched wire. $\sigma^*/\sigma = 0$ corresponds to composites made with completely cut wires and $\sigma^*/\sigma = 1$ to composites made with undamaged wires.

5. Toughness Measurements

With the type of specimen described above, it proved very difficult to obtain accurate values of the work done after the UTS as a consequence of fibre pull-out. Reference to fig. 7 shows that the maximum load was often in the region of 2 to 3000 kg, when there is a considerable deflection

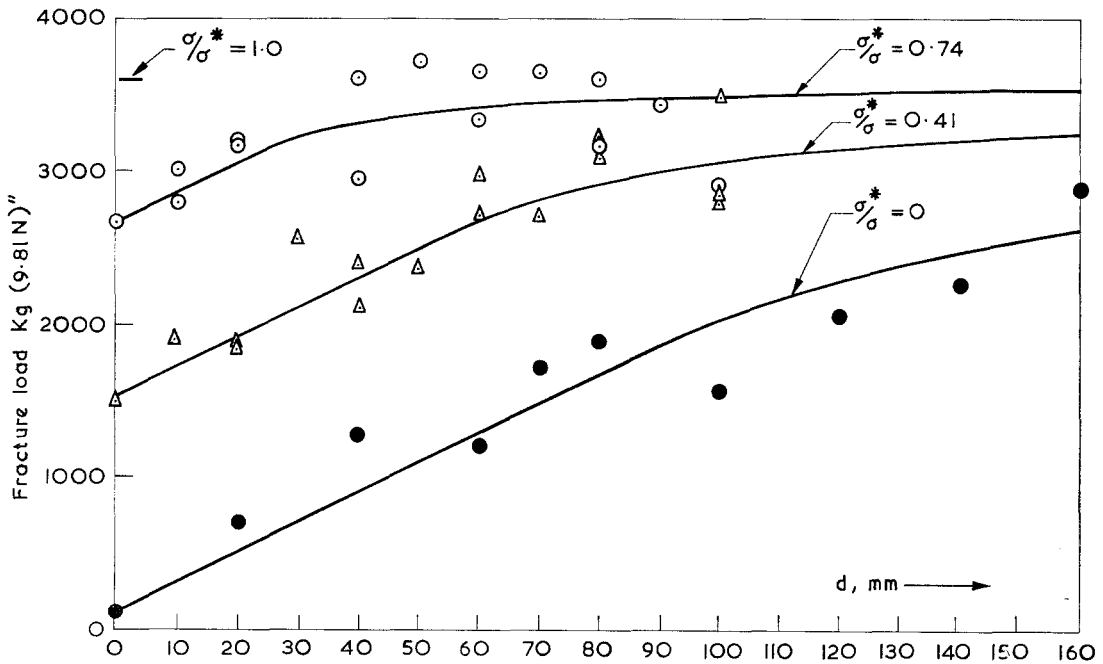


Figure 7 Variation of fracture load of 127-wire specimens with flaw spacing d for values of σ^*/σ of 0, 0.41, 0.78, and 1.0. The solid lines are theoretical plots from equations 5 and 9.

of the loading train, and thus considerable elastic energy stored in the testing machine. The "spring-back" of the grips at failure was sometimes sufficient to separate completely the broken pieces of the composite, which therefore registered a zero level of toughness by fibre pull-out. The problem was particularly severe in the case of the stronger composites, both because of the greater deflection of the machine, and because the stronger composites tended to be less tough.

In an effort to solve this problem, experiments were made upon a second type of specimen, sketched in fig. 5 (centre). In this type of specimen, modelled on those used by Tattersall and Tappin [3], the composite was cast as a rectangular block ($1.2 \times 1.2 \times 10$ cm) and the notch was cut afterwards with a fine saw. The specimens were tested in three-point bending, but although the problem of sudden failure was overcome, the full energy of pull-out was not developed, due to the excessively large displacement required to pull out fully some of the longer wires (fig. 8).

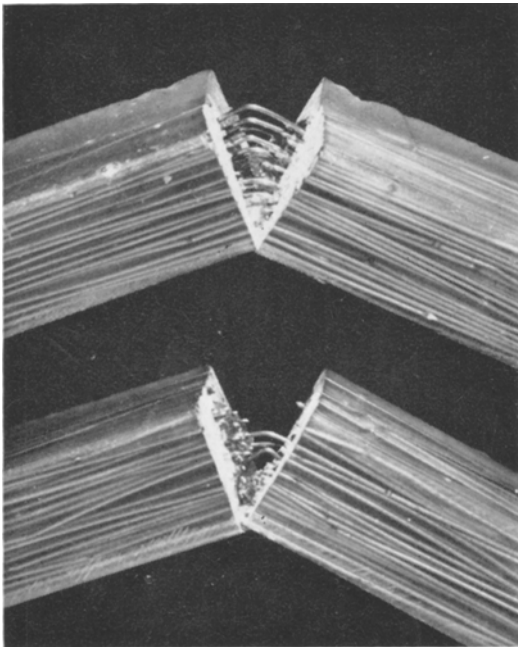


Figure 8 Fracture appearance of two typical bend specimens.

The final, and most successful, type of specimen is sketched in fig. 5 (bottom). This was again of dimensions $1.2 \times 1.2 \times 10$ cm, but contained only five wires, held by thin cardboard formers to prevent them sinking to the bottom of

the mould during casting. The centre spacer was made from a sheet of mica, so that on tensile testing the mica parted and left the wires spanning the gap. Care was taken with these specimens to position the weak points in the wires relative to the mica sheet in such a way as to give a distribution representative of random spacing.

These specimens suffered from none of the disadvantages of the previous specimens. Values of fracture energy due to fibre pull-out are shown in fig. 9 for the same values of σ^*/σ as the specimens in fig. 7.

6. Interpretation of Results

The theoretical treatment of the results is based upon the assumption that the failure crack in the matrix is approximately planar, and that each fibre spanning the crack can be treated in isolation from its neighbours. We consider a single fibre of uniform strength σ , except for a weak point, of strength σ^* at a distance y from the plane of the matrix crack. The stress in the fibre in the plane of the crack can reach a maximum value.

$$\sigma_{\text{MAX}} = \sigma^* + \frac{2}{r} \tau y \quad (1)$$

where τ is the static shear strength of the interface and r is the fibre radius before failure of the fibre at the weak point. If y is sufficiently large for σ_{MAX} to reach the failure stress of the undamaged fibre, then failure will occur at the plane of the matrix crack, at stress σ . The condition for failure at the weak point is thus:

$$y < \frac{(\sigma - \sigma^*)r}{2\tau} = \frac{(\sigma - \sigma^*)}{\sigma} \cdot \frac{l_c}{2} \quad (2)$$

If we consider a composite reinforced with fibres of strength σ having flawed regions of strength σ^* spaced a distance d apart, we have two possible conditions, depending upon whether d is less or greater than

$$d_{\text{CRIT}} = \frac{(\sigma - \sigma^*)}{\sigma} \cdot l_c \quad (3)$$

In the case where d is less than d_{CRIT} all fibres will be broken at weak points, giving rise to fibre pull-out. The failure stresses of the fibres in the plane of failure will lie uniformly between

$$\sigma^* \text{ and } \left(\sigma^* + \frac{2\tau}{r} \cdot \frac{d}{2} \right) \quad (4)$$

so that the mean apparent breaking stress of the fibres spanning the crack will be

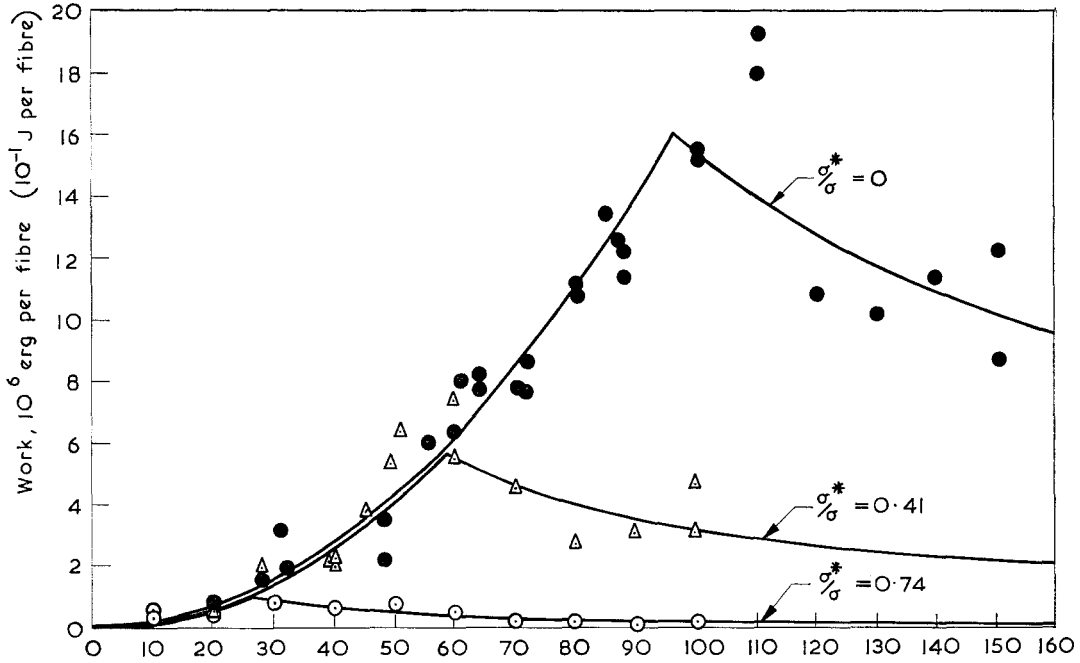


Figure 9 Variation of fracture work per wire for five-wire specimens with flaw spacing d for values of σ^*/σ of 0, 0.41 and 0.78. The solid lines are theoretical plots from equations 8 and 11.

$$\bar{\sigma} = \sigma^* + \frac{\tau d}{2r} = \sigma^* + \frac{d\sigma}{2l_c} \quad (5)$$

The lengths of fibre pulled out will vary uniformly from zero to $d/2$. The work done in pulling out a single fibre of length z is

$$w = \int_0^z P dy = \int_0^z 2\pi r \tau_s y dy \quad (6)$$

where τ_s is the shear friction stress during fibre pull-out. The mean value for a population with lengths zero to z is:

$$\begin{aligned} & \frac{1}{z} \int_0^z \pi r \tau_s z^2 dz \\ &= \frac{\pi r \tau_s}{3} z^2. \end{aligned} \quad (7)$$

In the case under consideration, z will vary between zero and $d/2$, giving the mean work done per fibre as:

$$\bar{w} = \frac{\pi r \tau_s}{3} \cdot \frac{d^2}{4} = \frac{\pi r \tau_s d^2}{12} \quad (8)$$

In the case where d is greater than d_{CRIT} (equation 3), only a fraction d_{CRIT}/d of the fibres are broken at flaws, while the rest break at stress σ .

The fibres which break at weak points have failure stresses lying with equal probability between σ^* and σ , the mean value thus being $(\sigma + \sigma^*)/2$.

The mean breaking stress of all the fibres in the composite is therefore

$$\begin{aligned} \bar{\sigma} &= \left(1 - \frac{d_{CRIT}}{d}\right) \sigma + \frac{d_{CRIT}}{d} \left(\frac{\sigma + \sigma^*}{2}\right) \\ &= \sigma - \frac{d_{CRIT}}{2d} (\sigma - \sigma^*) \end{aligned}$$

and so, using equation 3,

$$\bar{\sigma} = \frac{l_c}{2d} \frac{(\sigma - \sigma^*)^2}{\sigma} \quad (9)$$

As noted above, only the fraction d_{CRIT}/d of the fibres fracture at weak points, and contribute to the pull-out energy. They have lengths from zero to $d_{CRIT}/2$, and a mean length $d_{CRIT}/4$. The average work of fracture of these fibres, following the method leading to equation 8, is

$$\bar{w} = \frac{\pi r \tau_s}{12} (d_{CRIT})^2 \quad (10)$$

but since they represent a fraction of all the fibres, the mean work of fracture for all fibres is

$$\bar{w} = \frac{d_{\text{CRIT}}}{d} \cdot \frac{\pi r \tau_s}{12} (d_{\text{CRIT}})^2$$

$$\bar{w} = \left(\frac{\sigma - \sigma^*}{\sigma} \cdot l_c \right)^3 \cdot \frac{\pi r \tau_s}{12 d} \quad (11)$$

The theory predicts that the reinforcing capability (i.e. the mean breaking stress of the fibres *in the composite*) of these fibres is equal to the strength of the flawed regions for very small values of d , and increases linearly with d until the spacing becomes equal to d_{CRIT} (equation 3). Thereafter, the reinforcing capacity rises less rapidly, making an asymptotic approach to the strength of the unweakened fibre. This behaviour is sketched in fig. 10.

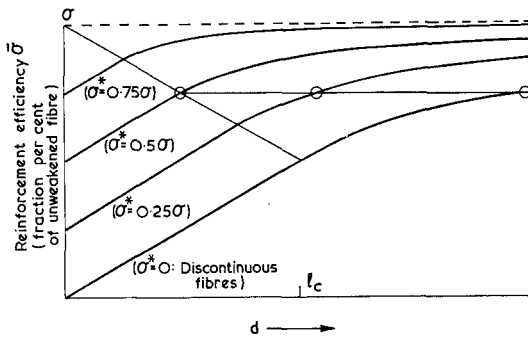


Figure 10 The variation of composite strength with d for values of $\sigma^*/\sigma = 0, 0.25, 0.5$ and 0.75 calculated from equations 5 and 9. The horizontal line joins three composites of equal strength whose toughnesses are represented in fig. 11.

The energy due to fibre pull-out, w , increases parabolically from zero with d until d_{CRIT} . Thereafter it decreases, being proportional to $1/d$. This behaviour is sketched in fig. 11.

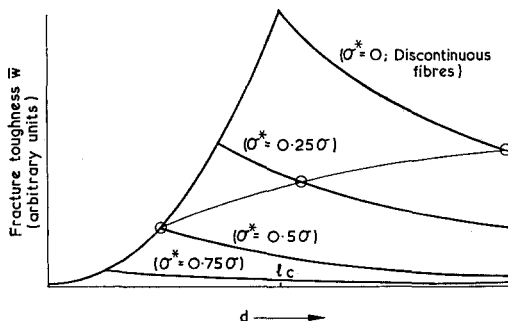


Figure 11 The variation of composite toughness with d for values of $\sigma^*/\sigma = 0, 0.25, 0.5$ and 0.75 calculated from equations 8 and 11. The line joining the three circled values is calculated from equation 17.

We note that equations 5 and 9, and 8 and 11, reduce to the same expressions when $d = d_{\text{CRIT}}$. When $\sigma^* = 0$ (discontinuous fibres), equations 5 and 9 reduce to the well-known equations of Kelly and Tyson for the strength of discontinuously-reinforced composites [4, 5], while equations 8 and 11 also reduce to forms previously derived (1, 2, 6) for the work due to fibre pull-out in composites with discontinuous fibres.

The experiments on pull-out of single fibres (fig. 4) gave values of the static strength of the interface (τ) (upper line), and also of the shear resistance during sliding (τ_s) (lower line). τ was calculated as the maximum load on the fibre divided by the area of contact between fibre and matrix. From the former, a value of l_c was obtained, and hence, with the known values of σ and σ^*/σ used in the experiments, theoretical lines were constructed using equations 5 and 9, and were applied to fig. 7 (q.v.). There is good agreement of theory with experiment.

Similarly, the value of the sliding friction stress τ_s was substituted in equations 8 and 11, along with the known values of l_c and σ^*/σ noted above, and theoretical lines were drawn on fig. 9. Again, good agreement between theory and experiment is seen, with the exception that the results are somewhat erratic in the region $d \sim d_{\text{CRIT}}$. This was because the most deeply embedded fibres were just about to break rather than pull out. While this had very little effect on the strength of the composites, it had a large effect on the work to fracture; in a five-fibre composite, the difference between the longest fibre just failing or just pulling out made a very large difference in the measured fracture energy.

7. Discussion

In general, the theory agrees well with the experimental results. An alternative view of the failure process can, however, be put forward if one considers the slow loading of an un-notched composite reinforced by the type of continuous but flawed fibre considered above. If the fibres run from end to end of the specimen, equal strain conditions must occur, and the fibres must be equally loaded. It follows, therefore, that when a mean fibre stress of σ^* is reached, all the weak points should fail and the composite should behave as if reinforced with discontinuous fibres. This can lead either to a "yield point" or to immediate failure of the composite, depending upon whether the strength of the "discontinuously reinforced" composite produced by failure

of all the flaws is greater or less than σ^* . The condition for failure to occur immediately after failure of the weak points (at stress σ^*) is:

$$d < \frac{2l_c\sigma^*}{\sigma} \quad \left(0 < \sigma^* < \frac{\sigma}{2}\right)$$

$$\text{or } d < \frac{l_c\sigma}{2(\sigma - \sigma^*)} \quad \left(\frac{\sigma}{2} < \sigma^* < \sigma\right).$$

The significance of these expressions can be illustrated graphically. Referring to fig. 10, a horizontal line drawn from σ^* to its intersection with the line corresponding to $\sigma^* = 0$ (the strength of discontinuous composites) defines the critical flaw spacing d^* . Composites reinforced with fibres having flaw spacings less than d^* would be expected to fail catastrophically at a stress σ^* , while composites having fibres with flaw spacings greater than d^* would be expected to show a yield point at σ^* , and thereafter behave as discontinuously-reinforced composites.

This behaviour did not occur in our experiments, as is evident from the results shown in fig. 7. If it had been the case, the strength values would have remained constant at the value σ^* until the value d^* had been reached, after which they would have risen, following the line corresponding to reinforcement with discontinuous fibres ($\sigma^*/\sigma = 0$). The observed behaviour, showing an immediate rise in composite strength above σ^* for non-zero values of d , indicates that the mechanism proposed above was not operating in our composites. This could be a consequence of the residual ductility of the metal near the flaw. If the flawed region could elongate slightly while still carrying a stress σ^* , then failure would not occur at a strain corresponding to an elastic stress of σ^* in the fibres. The condition that the stress in the flaw should not exceed σ^* while the stress in the undamaged wires rises to some higher value requires that the deficit in elastic strain along the flawed fibre be made up by a plastic strain at the weak point. The required plastic elongation can be calculated for the two conditions ($d > d_{\text{CRIT}}$) as follows:

(i) $d < d_{\text{CRIT}}$: At failure, the maximum stress in the fibre is realised mid-way between the flaws, and is of magnitude

$$\sigma_{\text{MAX}} = \sigma^* + \frac{d\sigma}{l_c} \quad (14)$$

The overall elongation of the composite must therefore be at least equal to σ_{MAX}/E , although the stress in the fibre lies between σ^* and σ_{MAX} .

The deficit in elastic elongation of the fibre between two weak points is therefore

$$\delta e = \frac{\sigma_{\text{MAX}} - \sigma^*}{2} \cdot \frac{d}{E} = \frac{d^2\sigma}{2El_c} \quad (15)$$

(ii) $d > d_{\text{CRIT}}$: In this case, the composite strain at failure equals σ/E , corresponding to the failure of the undamaged fibre, and the deficit in elastic elongation between two weak points is therefore

$$\delta e = \frac{(\sigma - \sigma^*)}{E} \cdot \frac{(\sigma - \sigma^*)}{\sigma} \cdot \frac{l_c}{2}$$

$$= \frac{(\sigma - \sigma^*)^2}{2E\sigma} \cdot l_c \quad (16)$$

Considering our experimental results, the maximum local elongation would have been expected when $\sigma^*/\sigma = 0.41$ and $d = d_{\text{CRIT}}$. In this case, substitution in equations 15 or 16 gives $e = 0.34$ mm. Thus, if the reinforcing wire were capable of a local elongation of 0.34 mm in the region of the flaw, the composite would not be expected to show a sudden failure at an average fibre stress σ^* , but would fail at a stress given by equations 5 or 9.

Considering the inherent ductility of the phosphor-bronze wire used in these experiments, this elongation, being less than a fibre diameter, is just possible. The fact that the experimental points agree with the predictions of equations 5 and 9 supports this view, although subsequent examination of the broken test pieces did not show any definite evidence of large local elongations at the flaws. It should be borne in mind, however, that the elongation of 0.34 mm calculated above is a maximum value of all experiments, and that in most cases, the elongation calculated from equations 15 and 16 is considerably smaller.

It would be interesting to extend the theory to deal with fibres in which d and σ^* do not have constant values, as is the case in real composites. This clearly requires a statistical approach, which is beyond the scope of this paper. The following very general observations can, however, be made. A composite having flaws of constant strength, yet spaced randomly, could be regarded as being made of sub-composites, each with the flaw spacing in a small range, d to $d + \delta d$. The strength and mean length of fibre pulled out during fracture could be identified for each of these sub-composites, and an appropriate summation procedure used to add the contributions from each of the sub-units. Reference to figs. 10 and 11 shows that in the region $d < d_{\text{CRIT}}$, the

strength will be accurately found by using the mean spacing between flaws, and the toughness by using the RMS value. In the region $d > d_{\text{CRIT}}$ the mean value of the flaw spacing will somewhat underestimate both strength and toughness, while in the region $d \sim d_{\text{CRIT}}$, the toughness may be considerably overestimated by substituting the mean flaw spacing into equations 8 or 11.

Extension of these arguments to the case of constant flaw spacing, but variable flaw strength, and hence to composites with neither d nor σ^* constant can be envisaged, but must be much more speculative until the failure process is more completely understood. In particular, the question of whether the weak points fail at, or before general yield, must be examined. This could be particularly important when there is a wide spread in the values of σ^* .

8. Conclusions

The strength and toughness of composites reinforced with flawed fibres have been examined in the case where the flawed regions were of constant strength, and were separated by a constant distance.

A theory has been put forward which adequately explains the experimental results, although its application to systems reinforced by completely brittle fibres should be investigated further.

One of the aims of the work was to determine the conditions for simultaneous maxima of strength and toughness. An examination of figs. 10 and 11 shows that there are no advantageous conditions in the region $d < d_{\text{CRIT}}$. In the region $d > d_{\text{CRIT}}$, the combination of equations 9 and 11 gives

$$\bar{w} = \left(\frac{2(\sigma - \bar{\sigma})}{\sigma} \cdot l_c \right)^{3/2} \frac{\pi r \tau_s d^{1/2}}{12} \quad (17)$$

$$\text{or} \quad \bar{w} = \frac{(\sigma - \sigma^*)}{\sigma^2} \cdot (\sigma - \bar{\sigma}) \frac{l_c^2 \pi r \tau_s}{6}. \quad (18)$$

These show that, for *constant composite strength*, the toughness increases linearly with $(\sigma - \sigma^*)$, and also in proportion to $d^{1/2}$. To illustrate this, three circles have been placed on fig. 10 to represent conditions giving three composites of the same strength. The toughness of these same composites are shown in fig. 11, the line linking them being given by equation 17. *Composites of the maximum toughness for given strength will always be found when $\sigma^* = 0$, i.e. for discontinuous fibres. The maximum toughness under any conditions occurs when the fibres are discontinuous and of length l_c .*

Acknowledgements

The author is grateful for the assistance of D. G. Gladman in preparing and testing the composites to Dr A. Kelly for pointing out the inconsistency discussed in section 7 and to members of the DIMS Composite Materials Section, NPL, for many helpful discussions.

References

1. A. H. COTTRELL, *Proc. Roy. Soc. A* **282** (1964) 2.
2. A. KELLY, *ibid* 63.
3. H. G. TATTERSALL, and G. TAPPIN, *J. Mater. Sci.* **1** (1966) 296.
4. A. KELLY, and W. R. TYSON, *Proc. 2nd International Materials Symposium, California, 1964* (J. Wiley, New York and London).
5. A. KELLY and G. J. DAVIES, *Met. Revs.* **10** (1965) 37.
6. A. KELLY "Strong Solids" (Clarendon Press, Oxford, 1966) p. 161.

Received 2 April and accepted 14 May 1970.